



## PAPER

## Modelling anomalous diffusion in semi-infinite disordered systems and porous media

## OPEN ACCESS

## RECEIVED

12 September 2022

## REVISED

18 November 2022

## ACCEPTED FOR PUBLICATION

29 November 2022

## PUBLISHED

9 December 2022

Original Content from  
this work may be used  
under the terms of the  
[Creative Commons  
Attribution 4.0 licence](#).

Any further distribution  
of this work must  
maintain attribution to  
the author(s) and the title  
of the work, journal  
citation and DOI.

Ralf Metzler<sup>1,2,\*</sup> , Ashish Rajyaguru<sup>3</sup> and Brian Berkowitz<sup>4</sup> <sup>1</sup> Institute for Physics & Astronomy, University of Potsdam, Potsdam 14476, Germany<sup>2</sup> Asia Pacific Centre for Theoretical Physics, Pohang 37673, Republic of Korea<sup>3</sup> Paul Scherrer Institut, 5232 Villigen, Switzerland<sup>4</sup> Department of Earth and Planetary Sciences, Weizmann Institute of Science, Rehovot 7610001, Israel

\* Author to whom any correspondence should be addressed.

E-mail: [rmetzler@uni-potsdam.de](mailto:rmetzler@uni-potsdam.de)**Keywords:** diffusion, anomalous diffusion, breakthrough curves, constant boundary concentration**Abstract**

For an effectively one-dimensional, semi-infinite disordered system connected to a reservoir of tracer particles kept at constant concentration, we provide the dynamics of the concentration profile. Technically, we start with the Montroll–Weiss equation of a continuous time random walk with a scale-free waiting time density. From this we pass to a formulation in terms of the fractional diffusion equation for the concentration profile  $C(x, t)$  in a semi-infinite space for the boundary condition  $C(0, t) = C_0$ , using a subordination approach. From this we deduce the tracer flux and the so-called breakthrough curve (BTC) at a given distance from the tracer source. In particular, BTCs are routinely measured in geophysical contexts but are also of interest in single-particle tracking experiments. For the ‘residual’ BTCs, given by  $1 - P(x, t)$ , we demonstrate a long-time power-law behaviour that can be compared conveniently to experimental measurements. For completeness we also derive expressions for the moments in this constant-concentration boundary condition.

**1. Introduction**

Classical Brownian motion, or pedesis, the random motion of inert particles suspended in a simple liquid or gas, is characterised by the linear time dependence  $\langle x^2(t) \rangle = 2K_1 t$  of the mean squared displacement (MSD) with the diffusion coefficient  $K_1$  [1, 2], as experimentally verified by Nordlund in 1914 [3]. The spreading of Brownian particles in space, in a macroscopically one-dimensional domain, is described by the Gaussian law  $P(x, t) = (4\pi K_1 t)^{-1/2} \exp(-x^2/[4K_1 t])$  for the probability density function (PDF) [1, 2, 4]. Brownian motion can be modelled in terms of stochastic forces (noise) [5–7] or as the continuum limit of a random walk [8–10], and its perpetuity follows from energy equipartition [11].

Deviations from the linear time dependence of the MSD of Brownian motion are widespread across the disciplines [12–18] and frequently have the power-law dependence  $\langle x^2(t) \rangle \simeq K_\beta t^\beta$ , in terms of the anomalous diffusion exponent  $\beta$  and the generalised diffusion coefficient  $K_\beta$  of physical dimension  $\text{length}^2/\text{time}^\beta$  [10, 16, 19]. Such anomalous diffusion can be subdiffusive ( $0 < \beta < 1$ ) or superdiffusive ( $\beta > 1$ ). Examples of anomalous diffusion are charge carrier motion in amorphous semiconductors [20, 21], passive tracer particle motion [22, 23] and molecular motor-driven motion in biological cells [24–26], motion of particles in crowded environments such as biological membranes [27–29] or dense liquids [30, 31], chemical migration in porous media [32, 33], as well as transport in structured environments such as gels [26, 34–36]. Even rather simple systems show distinct anomalous diffusion features, e.g. relatively small drug molecules between two silica slabs [37] (compare the anomalous diffusion modelling of drug release from a slab geometry in [38]). And yet, in naturally occurring porous media such as soils and rock formations, as well as in natural and engineered pore structures such as membranes and in catalytic systems, diffusion of chemical species is almost invariably modelled as a Brownian process with linear time

dependence of the MSD, or in other words, in terms of Fick's law [39, 40]; these disciplines thus completely ignore the possible—or likely—occurrence of anomalous diffusion in such heterogeneous, disordered media. In this context we allude to literature reporting on fractional versions of Fick's law [41–46].

Anomalous diffusion is non-universal in the sense that an empirical MSD-exponent  $\beta$  can emerge from distinctly different physical processes [16–19]. The best-known such stochastic processes include fractional Brownian motion (FBM) and the continuous time random walk (CTRW). FBM and the closely related generalised Langevin equation with power-law memory structure are based on Gaussian yet power-law correlated noise [47, 48]. These processes are stationary in increments, yet the emerging dynamics are highly non-Markovian. CTRWs are 'semi-Markovian' renewal processes [49] based on independent and identically distributed random variables for the length of each step and the sojourn intervals in between consecutive steps (or, alternatively, the travel times of the transitions) [16, 18–20, 50]. CTRWs with power-law waiting time (or transition time) or jump length densities can be mapped onto time- and space-fractional diffusion equations [16, 51–57]. We note that instead of a particle switching between sojourn periods and steps, one can also treat transient immobilisation in so-called mobile-immobile models (MIMs) [58–60] (see also [61, 62]). Using these residence times one could thus derive a generalised application of CTRW in fractional MIM models [63, 64].

CTRW subdiffusion is inherently non-Gaussian [16]. However, the Gaussianity of the process in complex systems cannot be used solely to rule out intrinsically Gaussian processes such as Brownian motion or FBM, as heterogeneous parameters in intrinsically disordered systems can effect non-Gaussianity in FBM and the generalised Langevin equation [65, 66], similar to two-state processes [22]. To distinguish between different stochastic mechanisms, a number of complementary statistical observables [18, 37, 67] or machine-learning approaches [68–73] need to be applied.

In the context of tracer motion in soils and aquifers, the CTRW framework has been developed, adapted and applied extensively to anomalous *transport* in porous media, i.e. for systems particularly relating to hydrology and petroleum engineering, wherein there is an underlying advective fluid velocity (bias) that carries chemical species [74]. The theoretical models and their solutions have been confirmed by extensive comparison to both experiments (laboratory and field scale) [75–77] and numerical simulations [78–80].

Here, we now apply the CTRW framework to anomalous *diffusion*, i.e. systems for which there is no bias, only pure diffusion, in disordered and porous media. In this context, we consider the same types of porous media—rocks, soils, sand—as for the biased case. Significantly, explicit solutions for anomalous diffusion have to date not been developed in the context of experimentally accessible scenarios as we develop here. In such scenarios the physical observable is not the MSD, as this is difficult to measure. Alternatives for directly accessible observables are electrical currents in wide but finite amorphous semiconductors [20, 21], equivalent to the charge carrier flux, or outflow concentrations (breakthrough curves (BTCs)) as functions of time [81, 82]. Here the initial conditions are typically point-like ( $\delta$ -type initial concentration profiles). Models for such experimental scenarios were developed in the presence of external bias (electrical current, hydrological bias) [20, 82], including the case of aged CTRWs, when the experimental bias is switched on some time after the tracer particles are introduced [21, 83–85]. In absence of a bias, CTRWs were solved for both semi-infinite and finite domains, for  $\delta$ -initial conditions [86].

A word is in order on the modelling approach in terms of a CTRW, in which successive waiting times are considered to be statistically independent. The assumption of such independent waiting times is called the 'annealed limit' in physics literature [19]. In a real system with a fixed geometry, traversing a specific position in space (e.g. a small pore in which the particle is trapped for some time) will take a particle statistically the same transit time, i.e. spatial correlations in this 'quenched' disorder should occur. This is indeed known for one-dimensional systems such as the quenched energy model [19, 87], see also the discussion in [88]. However, an external bias driving the particle, on average, in one direction, already diminishes these effects. As here we consider a system with an effective flux from inlet to outlet boundary, this is the first justification to use the annealed limit approach with independent waiting times. The second justification comes from the fact that our system is only effectively one-dimensional, and the formulation as a function of  $x$  only can be considered as an average over a finite cross-section of the porous material. The real medium, that is, has a three-dimensional extension, i.e. the particles can take many different paths across the medium. The effective motion monitored along some linear axis therefore 'shuffles' a large number of waiting times, which should allow us to use the annealed limit.

We expect to identify anomalous diffusion in rocks, via future experiments, but readily available solutions against which quantitative comparisons can be made are currently unavailable. Somewhat surprisingly, despite extensive literature on the theory and modelling of anomalous diffusion in disordered media, studies have not focused on the development of models that can be matched to experimental measurements in a semi-infinite, effectively one-dimensional geometries with *constant-concentration boundary condition*. Moreover, while some diffusion experiments have been reported in the literature, these studies either provide

insufficient information and/or were designed on the assumption that diffusion is Fickian, so that there is currently no well-defined way to determine if these data exhibit anomalous diffusion [89–92]. Indeed, currently, most data are ‘force-fitted’ to the standard (Fickian) diffusion equation. Here we develop these anomalous diffusion solutions (spatial profile and BTCs), in the context of application to actual porous media experiments. We then compare the various solutions to show their sensitivity to model parameters, and conditions in which the resulting solutions are measurably distinct from those of Fickian diffusion.

## 2. Mathematical development and experimental observables

In this section we briefly review how anomalous diffusion is introduced in the CTRW framework and how the PDFs for normal and anomalous diffusion are related in an unbounded, one-dimensional domain. In the second subsection we then discuss how to construct the Brownian solution in a semi-infinite, one-dimensional domain with fixed boundary concentration. In the following section we then apply the CTRW generalisation to this half-space solution and analyse its behaviour in detail.

### 2.1. CTRWs and time-fractional diffusion equation

To model tracer motion in a disordered environment, we consider a CTRW process in a macroscopically one-dimensional domain, with a Gaussian jump length distribution defined via its Fourier transform  $\lambda(k) = \mathcal{F}\{\lambda(x)\} = \int_{-\infty}^{\infty} \lambda(x) \exp(ikx) dx = \exp(-\sigma^2 k^2/2)$  with variance  $\sigma^2$  and a power-law waiting or transition time density defined in terms of its Laplace transform  $\psi(s) = \mathcal{L}\{\psi(t)\} = \int_0^{\infty} \psi(t) \exp(-ut) dt = \exp(-[u\tau]^\beta)^5$ . In Fourier-Laplace space the PDF to find the particle at position  $x$  at time  $t$  after being released at  $x=0$  at time  $t=0$  is given by the Montroll–Weiss equation [50]

$$P(k, u) = \frac{1 - \psi(u)}{u} \frac{1}{1 - \lambda(k)\psi(u)}. \quad (1)$$

Here, we see that  $P(x, t)$  is normalised, i.e.  $\int_{-\infty}^{\infty} P(x, t) dx = 1$ , a relation corresponding to  $P(k=0, t)$  in Fourier space. Using the fact that  $\lambda(k=0) = 1$ , we see that  $P(k=0, u) = 1/u$ , which indeed corresponds to  $P(k=0, t) = 1$ . In our formulation, this PDF  $P(x, t)$  thus is the ‘relative concentration’.

Considering the diffusion limit  $x, t \rightarrow \infty$ , corresponding, more precisely, to having  $x \gg \sigma$  and  $t \gg \tau$  in terms of the intrinsic (typically microscopic) scales of the CTRW model, the corresponding PDFs of the jump lengths and waiting times can be expanded in the respective Fourier and Laplace domains for small  $k$  and  $u$ ,  $\lambda(k) \sim 1 - \sigma^2 k^2/2$  and  $\psi(u) \sim 1 - (u\tau)^\beta$  [16]. Introducing these forms into the Montroll–Weiss equation (1) and rearranging terms, after neglecting mixed terms of  $u$  and  $k^2$  we find

$$uP(k, u) - P_i(k) = -u^{1-\beta} K_\beta k^2 P(k, u), \quad (2)$$

where  $P_i(x) = \delta(x)$  with  $P(k) = 1$  is the initial condition for a single particle release at  $x=0$  at  $t=0$ . The anomalous diffusion coefficient is defined as  $K_\beta = \sigma^2/[2\tau^\beta]$  in terms of the parameters of the jump length and waiting time PDFs [16, 52].

For  $\beta=1$ , the waiting time PDF in time domain reduces to the sharply peaked form  $\psi(t) = \delta(t - \tau)$ , i.e. every jump has the same waiting time  $\tau$ . From equation (2) we can then obtain directly the normal diffusion equation  $\partial P(x, t)/\partial t = K_1 \partial^2 P(x, t)/\partial x^2$  by identification of  $\mathcal{F}^{-1}\{-k^2 P(k, u)\} = \partial^2 P(x, t)/\partial x^2$  and  $\mathcal{L}^{-1}\{uP(k, u) - P_i(k)\} = \partial P(x, t)/\partial t$  via standard theorems of Fourier and Laplace transforms. The solution in this case is the Gaussian [16, 51]

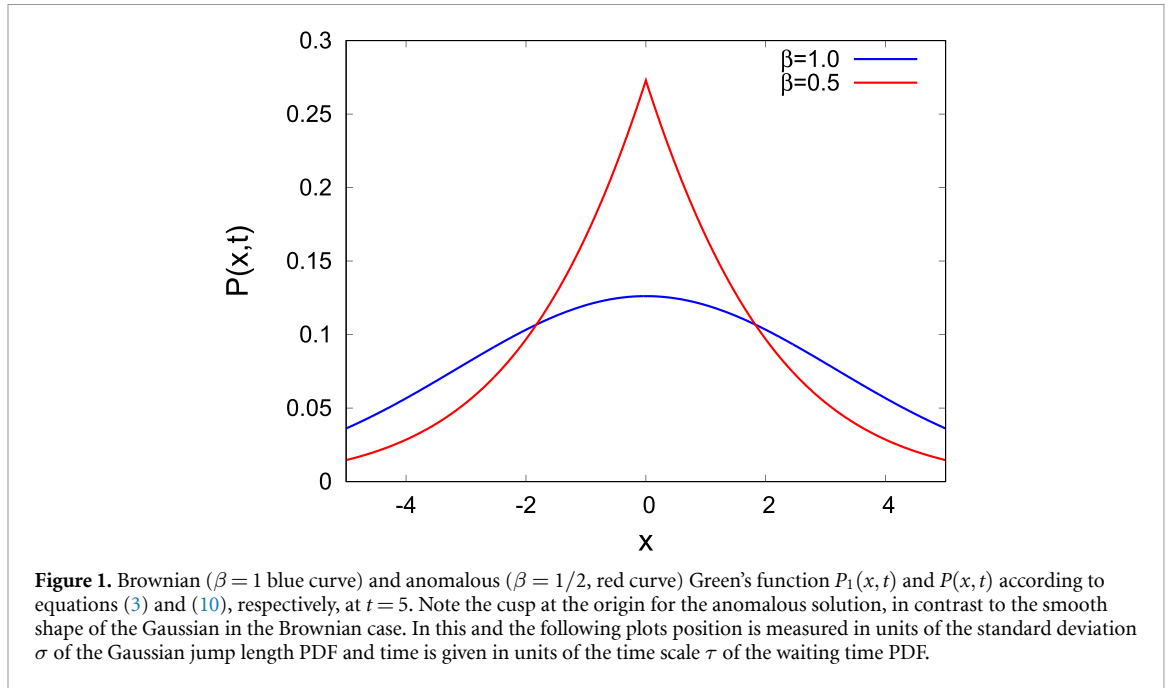
$$P_1(x, t) = \frac{1}{\sqrt{4\pi t}} \exp\left(-\frac{x^2}{4K_1 t}\right). \quad (3)$$

In figure 1 we display this ‘Green’s function’, i.e. the PDF for  $\delta$ -initial condition along with the generalised case for  $\beta=1/2$ , constructed below.

For  $0 < \beta \leq 1$ , equation (2) includes a term of the form  $u^{1-\beta} k^2 P(k, u)$ , where  $u^{1-\beta} P(k, u)$  represents the Laplace transform of the fractional differential of  $P(k, t)$  in time space [16, 27, 93]. Using this fact, Fourier-Laplace inversion of (2) leads to the time-fractional diffusion equation [16, 27, 51, 52, 54–57]

$$\frac{\partial}{\partial t} P(x, t) = {}_0D_t^{1-\beta} K_\beta \frac{\partial^2}{\partial x^2} P(x, t), \quad (4)$$

<sup>5</sup> Here we use the conventional notation that the transform of a function is solely expressed by the explicit dependence on the transformed variable, e.g.  $f(u) = \mathcal{L}\{f(t)\}$  and  $g(k) = \mathcal{F}\{g(x)\}$ .



in which the time-fractional derivative in the Liouville–Riemann sense is defined as [16, 93]

$${}_0D_t^{1-\beta}P(x, t) = \frac{1}{\Gamma(\beta)} \frac{\partial}{\partial t} \int_0^t \frac{P(x, t')}{(t-t')^{1-\beta}} dt'. \tag{5}$$

This formulation in terms of a partial integro-differential equation has the distinctive advantage that boundary value problems can be solved quite easily, as we will demonstrate below. We note that in the presence of advection with speed  $v$ , the fractional diffusion equation (4) will feature an additional drift term, as detailed in [94]. In our case no such external driving is considered.

For ‘natural’ boundary conditions  $\lim_{|x| \rightarrow \infty} P(x, t) = 0$  and our sharp initial condition  $P_i(x) = \delta(x)$ , the second moment of  $P(x, t)$  can be checked easily from equation (4) via integration of  $x^2$  over space,  $\int_{-\infty}^{\infty} x^2 \cdot dx$ : the left hand side immediately produces  $(d/dt)\langle x^2(t) \rangle$ ; integration by parts twice on the right hand side leads to  $[2/\Gamma(\beta)]K_\beta(d/dt) \int_0^t (t-t')^{\beta-1} dt' = [2/\Gamma(\beta)]K_\beta(d/dt)t^\beta/\beta = 2t^{\beta-1}/\Gamma(\beta)$ . Using the initial condition  $x(0) = 0$  yields  $\langle x^2(t) \rangle = 2K_\beta t^\beta/\Gamma(1+\beta)$ . For ease of notation we will use reduced dimensional units in the following, obtained from re-scaling of space by  $x \rightarrow x/\sigma$  and of time by  $t \rightarrow t/[2\tau^\beta]$  such that  $K_\beta = 1$  in these units.

While for point-like initial conditions in a semi-infinite domain the fractional diffusion equation (4) can be solved explicitly in terms of Fox  $H$ -functions [16, 86], the additional averaging necessary to consider the constant-concentration boundary condition could not be performed. We therefore resort to an alternative approach based on so-called subordination which is equivalent to the fractional diffusion equation (4) [95]. This approach allows us to obtain the quantities of interest as a transform of the known Brownian solution. The concept of subordination [96] in this case can be understood if we rephrase a CTRW in terms of two coupled continuous-time stochastic equations,  $dx(s)/ds = \eta(s)$  and  $dt(s)/ds = \tau(s)$ , where  $s$  is the path parameter (‘arc length’) along the particle trajectory,  $\tau$  are the randomly distributed waiting (or transition) times, and  $\eta$  are random jump lengths [97]. Here the equation for  $x(s)$  corresponds to the regular Langevin equation if, as we assume here, the distribution of the jump lengths  $\eta$  is sufficiently narrow and has a finite variance. The role of the path parameter  $s$  is the ‘number of steps’. The transformation equation for  $t(s)$  then connects random waiting times to each step and maps the dynamic  $x(s)$  to the ‘real’ process time  $t$  [98]. This temporal ‘subordination’ of the step number, sometimes also called internal clock time, to the time  $t$  measured in experiments, can then be rephrased for the density  $P(x, t)$  for a given  $\beta$ . If we denote the Brownian solution of the normal diffusion equation (i.e. for  $\beta = 1$ ) with  $P_1$ , the subordination relation can be phrased by rescaling in Laplace space [51] or in terms of the integral transformation [16, 99]

$$P(x, t) = \int_0^\infty \mathcal{E}_\beta(s, t) P_1(x, s) ds. \tag{6}$$

Here the kernel  $\mathcal{E}_\beta(s, t)$  is defined through its inverse Laplace transform as

$$\mathcal{E}_\beta(s, t) = \mathcal{L}^{-1} \{ u^{\beta-1} \exp(-u^\beta s); u \rightarrow t \}, \tag{7}$$

which defines the one-sided Lévy stable distribution  $L_\beta^+$  with an additional prefactor,

$$\mathcal{E}_\beta(s, t) = \frac{t}{\beta s} L_\beta^+ \left( \frac{t}{s^{1/\beta}} \right). \tag{8}$$

This kernel has the particularly simple form [16]

$$\mathcal{E}_{1/2}(s, t) = \frac{1}{\sqrt{\pi t}} \exp \left( -\frac{s^2}{4t} \right) \tag{9}$$

for  $\beta = 1/2$ . This form allows the exact evaluation of the subordination integral (6) to obtain the Green's function (the solution for the point-like initial condition  $P(x, 0) = \delta(x)$  for  $\beta = 1/2$ ,

$$\begin{aligned} P(x, t) &= \frac{1}{2^{3/2} \pi t^{1/4}} \Gamma \left( \frac{1}{4} \right) {}_0F_2 \left( \frac{1}{2}, \frac{3}{4}, -\frac{x^4}{256t} \right) \\ &= -\frac{|x|}{2\sqrt{\pi t}} {}_0F_2 \left( \frac{3}{4}, \frac{5}{4}, -\frac{x^4}{256t} \right) \\ &= -\frac{x^2}{16\sqrt{2\pi t^{3/4}}} \Gamma \left( -\frac{1}{4} \right) {}_0F_2 \left( \frac{5}{4}, \frac{3}{2}, \frac{x^4}{256t} \right), \end{aligned} \tag{10}$$

in terms of the generalised hypergeometric function  ${}_0F_2$ . The occurrence of the absolute value in  $x$  demonstrates the non-analytic behaviour of the PDF at the origin. This behaviour is characteristic of CTRW subdiffusion, for which the distinct cusp at the origin witnesses the slow decay of the initial condition  $P(x, 0) = \delta(x)$  with the sticking probability  $1 - \int_0^t \psi(\tau) d\tau$  that no jump has occurred until time  $t$  [10, 16]. The Green's function (10) is displayed in figure 1. Similarly, exact forms for  $\mathcal{E}_\beta(s, t)$  can be obtained for other rational numbers of  $\beta$ , such as  $\beta = 1/2, 1/3, 2/3$ , or  $3/4$  [16]. If other  $\beta$  values need to be evaluated, the corresponding form of  $P(x, u)$  in Laplace space is constructed by the subordination integral  $P(x, u) = \int_0^\infty \mathcal{E}_\beta(s, u) P_1(x, s) ds$ , and then inverted to time domain by numerical Laplace inversion. We note that in the context of transport this subordination concept was developed in [16, 51, 99] and was applied previously in [100].

We also note that so far we used the standard notation  $P(x, t)$  for the PDF of a Brownian particle which is normalised to unity,  $\int_{-\infty}^\infty P(x, t) dx = 1$ . In what follows we consider a macroscopic amount of tracer particles, whose distribution in space we express in terms of the concentration field  $C_\beta(x, t)$ .

### 2.2. Constant concentration boundary condition

In the above subsection we showed how the normal-diffusive solution can be related to the subdiffusive CTRW solution in terms of the subordination method. Here we now present the normal-diffusive form for the concentration field  $C(x, t)$  for a realistic experimental setup, in which a constant concentration  $C_0$  is applied at the inlet boundary of a macroscopically one-dimensional, horizontal porous medium column that is fully water-saturated. We assume that the outlet boundary is sufficiently far away to allow treatment of the system as having a semi-infinite support. Our strategy is to first solve the Brownian case,  $C_1(x, t)$ . In the next section we then employ the subordination concept to construct the density field  $C_\beta(x, t)$  and discuss its dynamic behaviour.

To proceed, we first outline, for pedagogical reasons, how to solve the normal diffusion equation for the step initial condition (in terms of the Heaviside function  $\Theta(x)$ )

$$C_0(x) = C_1(x, t = 0) = 2C_0 \Theta(-x) = \begin{cases} 2C_0, & x \leq 0 \\ 0, & x > 0 \end{cases}, \tag{11}$$

where we used the plateau value  $2C_0$  for reasons that become clear momentarily. The solution of the normal diffusion equation ( $\beta = 1$ ) for this specific initial value problem is simply given by the integral over the initial condition,

$$\begin{aligned} C_1(x, t) &= \int_{-\infty}^\infty C_i(x') \frac{1}{\sqrt{4\pi t}} \exp \left( -\frac{(x-x')^2}{4t} \right) dx' \\ &= \frac{2C_0}{\sqrt{4\pi t}} \int_{-\infty}^0 \exp \left( -\frac{(x-x')^2}{4t} \right) dx'. \end{aligned} \tag{12}$$

Here we used the fact that the Gaussian  $(4\pi t)^{-1/2} \exp(-[x-x']^2/[4t])$  is the Green's function of the diffusion equation (i.e. the solution for the  $\delta$ -initial condition  $C_i(x) = C_0\delta(x-x')$ ) and that the solution for a general initial condition can be obtained in the form (12).

Now we use the definition of the error function,

$$\operatorname{erf}(z) = \frac{2}{\sqrt{\pi}} \int_0^z e^{-\zeta^2} d\zeta, \quad (13)$$

which has the specific values  $\operatorname{erf}(0) = 0$  and  $\operatorname{erf}(\infty) = 1$ , and is antisymmetric in the argument  $\operatorname{erf}(-z) = -\operatorname{erf}(z)$ . Moreover, the complementary error function is defined as  $\operatorname{erfc}(z) = 1 - \operatorname{erf}(z)$ . With this, we now find that for our initial condition (11),

$$C_1(x, t) = C_0 \operatorname{erfc}\left(\frac{x}{\sqrt{4t}}\right). \quad (14)$$

This means that the value of this solution is  $C_0$  at  $x = 0$  at all times, and thus this specific initial value problem solves the desired boundary value problem with constant concentration at the origin (note the simple factor  $1/2$  connecting the two problems). We display the solution (14) for the Brownian case in figure 2(a). Note that, as per construction, the value of  $C_1(x, t)$  is unity at  $x = 0$  and that the slope at  $x = 0$  is finite at all times.

Due to the contact with the 'tracer reservoir' at  $x = 0$ , the overall amount of tracer in the semi-infinite water column becomes a function of time. We can calculate the time-dependent cumulative tracer amount as

$$\mathcal{T}(t) = \int_0^\infty C_1(x, t) dx = \frac{2C_0}{\sqrt{\pi}} t^{1/2}, \quad (15)$$

i.e. it exhibits a square-root growth dependence. The relative mean

$$\langle x(t) \rangle = \frac{1}{\mathcal{T}(t)} \int_0^\infty x C_1(x, t) dx = \frac{\sqrt{\pi}}{2} t^{1/2} \quad (16)$$

of the concentration moves away diffusively (i.e. with  $t^{1/2}$ -scaling) from the boundary. Finally, the relative standard deviation is

$$\sqrt{\langle \Delta x^2(t) \rangle} = \sqrt{\langle x^2(t) \rangle - \langle x(t) \rangle^2} = \frac{1}{\mathcal{T}(t)} \int_0^\infty x^2 C_1(x, t) dx - \langle x \rangle^2 = \sqrt{\frac{16 - 3\pi}{12}} t^{1/2}. \quad (17)$$

The relative standard deviation versus the relative mean is thus a constant, reflecting that the concentration field is broad, as expected. In the next section we will show how to generalise the above quantities to the subdiffusive case.

### 2.3. BTCs and tracer flux

The principal measurable quantity in one-dimensional column experiments is the BTC, representing the (relative) concentration over time at a specific distance from the inlet boundary. Experimentally, this can be done through multiple boreholes placed at predetermined distances from the tracer inlet. On smaller scales, the time evolution of the concentration profile in porous objects, projected onto a linear co-ordinate, can be monitored by field gradient nuclear magnetic resonance [101]. We parenthetically note that, in principle, measurements based on direct image analysis of the spatial distribution of a coloured tracer diffusing in a quasi-two-dimensional flow cell could also be used to directly determine the value of the density  $C_1$  (or the generalised quantity  $C_\beta(x, t)$  we seek to model). However, to date, such visualisation experiments have not been reported, due largely to technical constraints and the limited resolution of detectable concentrations. While for Brownian motion the BTC follows the law (14) for a fixed value of  $x$ , we will discuss the behaviour of the generalised BTC in the next section.

Another experimental method to probe porous structures of moderate porosity is based on single-particle tracking methods, e.g. reported for diffusing nanoparticles in [102]. Apart from measuring local properties such as void space accessibility, this method can be used to optically measure the spreading of the tracer particles across the porous medium. In our scenario of a one-dimensional column coupled to a tracer particle reservoir, one way to measure the transport dynamics is to determine the 'flux' of tracer particles *across* a pre-determined distance from the reservoir, i.e. the net number of particles crossing the monitoring plane to the right and to the left per unit time. This flux is determined via the relation

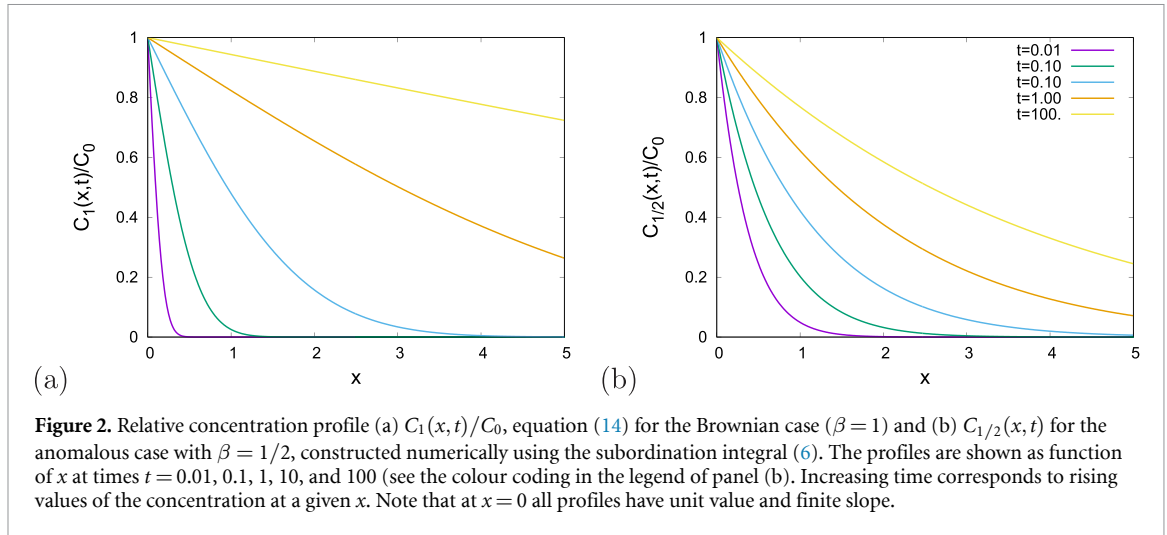


**Figure 2.** Relative concentration profile (a)  $C_1(x,t)/C_0$ , equation (14) for the Brownian case ( $\beta = 1$ ) and (b)  $C_{1/2}(x,t)$  for the anomalous case with  $\beta = 1/2$ , constructed numerically using the subordination integral (6). The profiles are shown as function of  $x$  at times  $t = 0.01, 0.1, 1, 10$ , and  $100$  (see the colour coding in the legend of panel (b)). Increasing time corresponds to rising values of the concentration at a given  $x$ . Note that at  $x = 0$  all profiles have unit value and finite slope.

$J_1(x,t) = -\partial C_1(x,t)/\partial x$ . Starting from our result (14) we then find<sup>6</sup>

$$J_1(x,t) = \frac{C_0}{\sqrt{\pi t}} \exp\left(-\frac{x^2}{4t}\right). \quad (18)$$

We note the power-law asymptote  $J_1(x,t) \simeq t^{-1/2}$  for  $t \gg x^2$ . This form contrasts the result  $(4\pi^{1/2}t^{3/2})^{-1} C_0 x \exp(-x^2/[4t])$  for the Gaussian density in unconfined space that features a  $t^{-3/2}$  asymptote. The fact that we have a non-zero flux at  $x = 0$  in our setting here is, of course, due to the constant-concentration boundary condition at the origin. As for fixed  $x = 0$  the concentration field is constantly building up, the concentration gradient becomes smaller and the (net) flux decreases over time. Remarkably, the flux (18) is independent of the initial position  $x_0$ , in contrast to the case of an initial  $\delta$ -pulse in an infinite geometry.

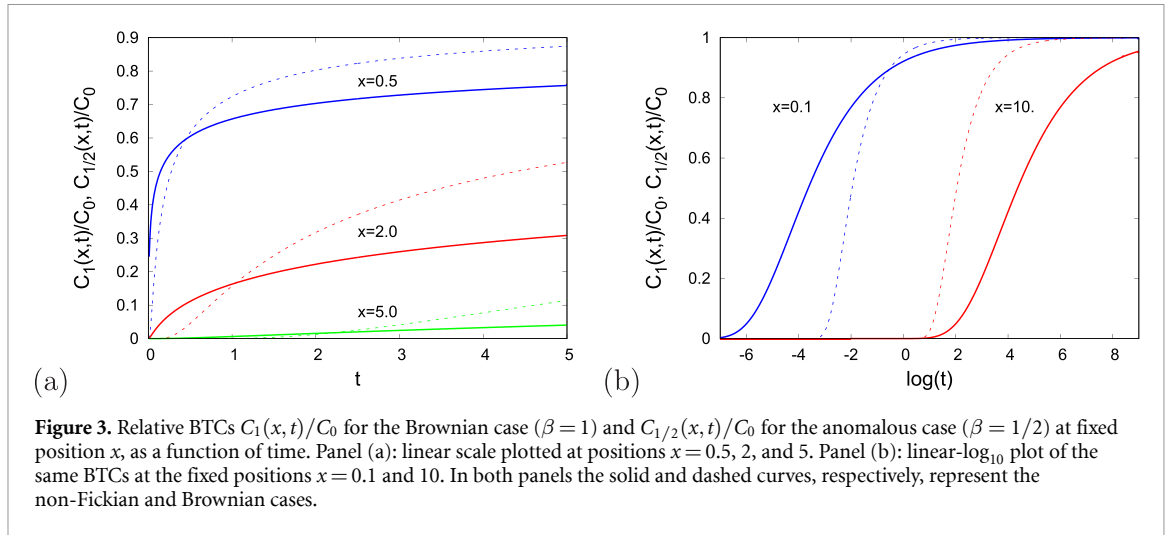
### 3. Solutions, results, analysis

In section 2 we demonstrated how the PDF for free Brownian motion can be used to construct the PDF for anomalous diffusion using the subordination method. There  $P(x,t)$  could be expressed in terms of the generalised hypergeometric function  ${}_0F_2$  in equation (10). For our experimental case with a constant-concentration boundary condition we could not find an explicit solution and therefore resort to numerical evaluations, constructed from the analytical Brownian result (14) together with the subordination law (6) for specific values of the anomalous diffusion exponent  $\beta$ . The integral in relation (6) is evaluated using the `NIntegrate` function of Mathematica [103]. We also use asymptotic scaling analyses to derive the scaling exponents for the ‘residual BTC’ defined below, which in many cases will be the relevant behaviour for the analysis of experimental data. These will allow a direct determination of the anomalous diffusion exponent  $\beta$ , the only adjustable model parameter in our non-dimensional units.

#### 3.1. Spatial concentration profiles and moments

Figure 2(a) shows the relative concentration profile  $C_1(x,t)/C_0$  for the Brownian case ( $\beta = 1$ , equation (14)) as function of  $x$  for different times. All curves meet at  $C_\beta(0,t) = C_0$ , the concentration fixed by the boundary condition. At short times, the tracer has hardly penetrated into the sample ( $x > 0$ ), while at longer times the concentration profile at finite  $x$  clearly increases, driven by the constant flux into the system from the boundary. Figure 2(b) shows the anomalous case with  $\beta = 1/2$ , based on the subordination integral (6), with  $C_1$  taken from equation (14). It is seen that the transport is actually faster than for the Brownian case at short times, while at longer times the subdiffusive transport is distinctly slower. In fact, Lévy stable laws such as the waiting time density  $\psi(t)$  employed here have a long tail and thus produce occasional, very long waiting times. Concurrently, however, they are also more concentrated around the origin, thus giving rise to a higher likelihood of short waiting times than a Poisson process. This property can also be seen for the BTCs below.

<sup>6</sup> Note that the flux  $J_1$  is the quantity entering the continuity equation in differential form, for the particle density. Also note that in non-reduced dimensions, the flux has the form  $J_1 = -K_1 \partial C_1(x,t)/\partial x$  and thus has dimensions of mass over time.



The shapes of the concentration profiles in the direct comparison between panels (a) and (b) of figure 2 naturally differ between the normal and anomalous cases. However, from a single or a series of profiles it is not straightforward to deduce the anomalous diffusion exponent, or even to decide whether the observed dynamics is anomalous or not. Even for the idealised case considered here, without measurement errors, this is due to the rather similar, fully convex shape. We will see similar features for the BTCs. However, the residual BTCs have a power-law asymptote, from which one can unambiguously determine the value of  $\beta$ .

For specific measurements an alternative way to determine the anomalous diffusion exponent  $\beta$  is to measure the moments associated with the transport dynamics. We here generalise the Brownian results (15)–(17), finding

$$\mathcal{I}_\beta(t) = \int_0^\infty C_\beta(x, t) dx = \frac{C_0}{\Gamma(1 + \beta/2)} t^{\beta/2}. \tag{19}$$

The square-root growth in time in the Brownian case, equation (15), is replaced by a scaling with  $t^{\beta/2}$ . To calculate the relative moments, we use the subordination method first for the moment and the normalisation  $\mathcal{I}(t)$  separately, and then divide the two results, obtaining for the relative mean

$$\langle x(t) \rangle_\beta = \frac{\Gamma(1 + \beta/2)}{\Gamma(1 + \beta)} t^{\beta/2}. \tag{20}$$

The relative standard deviation in the anomalous case is

$$\sqrt{\langle \Delta x^2(t) \rangle_\beta} = \sqrt{\langle x^2(t) \rangle_\beta - \langle x(t) \rangle_\beta^2} = \frac{(16 - 3\pi)\Gamma(1 + \beta/2)}{12\Gamma(1 + \beta)} t^{\beta/2}. \tag{21}$$

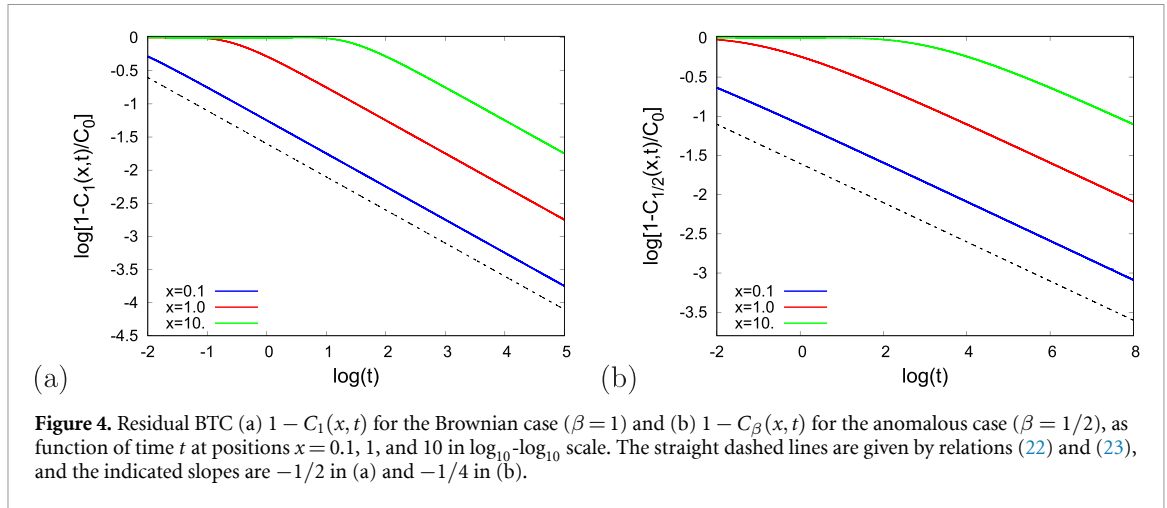
As in the Brownian case the standard deviation versus the mean is a constant.

### 3.2. Temporal BTCs

The BTCs for both normal and subdiffusion are shown in figure 3 in both linear and log–log scales. Comparison of the normal with the anomalous case demonstrates that the subdiffusive dynamic is faster at earlier times but then starts to lag behind the Brownian case, as expected according to the reasoning about Lévy stable laws above. Similar to our observation for the concentration profiles above, visual comparison of normal and subdiffusive cases shows a clear difference in the quantitative behaviour. However, it is critical to note that due to the gradual concave behaviour in these curves, from measurement of a single BTC it is not possible to clearly distinguish between the Brownian and subdiffusive cases, nor can one extract the value of the scaling exponent  $\beta$ .

A clear distinction between the Brownian and subdiffusive cases can be achieved by plotting the approach of the BTC to its plateau value, given by the ‘residual BTC’

$$1 - C_1(x, t)/C_0 = 1 - \operatorname{erfc}\left(\frac{x}{\sqrt{4t}}\right) \sim \frac{x}{\sqrt{\pi t}}. \tag{22}$$



This behaviour is easily deduced from equation (14), and we used the symbol  $\sim$  to denote the asymptotic behaviour for long times. Correspondingly for the behaviour for the subdiffusive case with  $\beta = 1/2$  one can find an exact expression in terms of generalised hypergeometric functions. However, here we only report the general asymptotic behaviour

$$1 - C_{\beta}(x, t)/C_0 \sim \frac{x}{\Gamma(1 - \beta/2)t^{\beta/2}}, \quad (23)$$

which follows directly from subordination of equation (22); the validity of subordinating the asymptotic behaviour directly can easily be verified by comparison with numerical evaluations of the subordination of the full expression. Here a clear scaling is found as a function of time in the asymptotic limit. The slope of this scaling law is related directly to  $\beta$ . This is corroborated in the log-log plots in figure 4 for  $\beta = 1/2$ . We emphasise that the long-time behaviour shows a proportionality to the position  $x$  at which the BTC is measured. This implies that the crossover time (such that  $x/t^{\beta/2} \ll 1$ ) to the asymptotic power-law is delayed for more distant  $x$  as compared to closer  $x$ . The power-law behaviour of the residual BTCs is our central result and easily amenable to analysis of experiments with constant boundary concentration.

### 3.3. Flux

Following the measurement of the net flux in single particle trajectory assays, as mentioned above, we now discuss the asymptotic behaviour of the tracer flux (18). In the case of normal (Fickian) diffusion, the long-time dependence of the flux (18) is

$$J_1(x, t) \sim \frac{C_0}{\sqrt{\pi t}}, \quad (24)$$

and, again using direct subordination of equation (24) for subdiffusion with  $\beta = 1/2$  this relation becomes

$$J_{1/2}(x, t) \sim \frac{\Gamma(1/4)C_0}{\sqrt{2\pi}t^{1/4}}. \quad (25)$$

For general  $\beta$ , we finally find

$$J_{\beta}(x, t) \sim \frac{C_0}{\Gamma(1 - \beta/2)t^{\beta/2}}. \quad (26)$$

The flux is portrayed in figure 5. In the log-log plot on the right the power-law asymptote becomes obvious. The power-law form of the flux in the long-time limit makes it amenable to easy extraction of the scaling exponent, and thus  $\beta$ , similar to the residual BTC. We note that for our constant-concentration boundary conditions, an exact solution for the flux can be obtained for the case  $\beta = 1/2$ , again in terms of generalised hypergeometric functions,

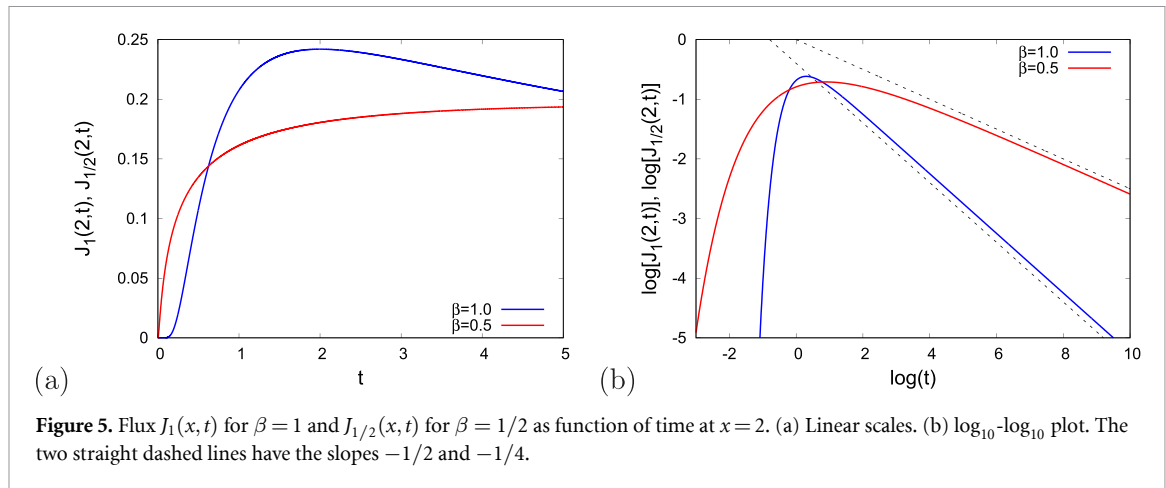


**Figure 5.** Flux  $J_1(x, t)$  for  $\beta = 1$  and  $J_{1/2}(x, t)$  for  $\beta = 1/2$  as function of time at  $x = 2$ . (a) Linear scales. (b)  $\log_{10}$ - $\log_{10}$  plot. The two straight dashed lines have the slopes  $-1/2$  and  $-1/4$ .

$$\begin{aligned}
 J(x, t) = & \frac{C_0}{\pi t^{1/2}} \left( \frac{t^{1/4}}{\sqrt{2}} \Gamma\left(\frac{1}{4}\right) {}_0F_2\left(\frac{1}{2}, \frac{3}{4}, -\frac{x^4}{256t}\right) \right. \\
 & - \sqrt{\pi}|x| {}_0F_2\left(\frac{3}{4}, \frac{5}{4}, -\frac{x^4}{256t}\right) \\
 & \left. - \frac{x^2}{8\sqrt{2}t^{1/4}} \Gamma\left(-\frac{1}{4}\right) {}_0F_2\left(\frac{5}{4}, \frac{3}{2}, -\frac{x^4}{256t}\right) \right), \quad (27)
 \end{aligned}$$

where we again use the hypergeometric function  ${}_0F_2$ . This function can be directly plotted in Mathematica.

## 4. Conclusions

We analysed the anomalous diffusion behaviour of passive tracer particles in a semi-infinite, macroscopically one-dimensional domain, whose inlet boundary is kept at a constant concentration. Experimentally, this case corresponds to a setup of a porous medium whose inlet interface is connected to a sufficiently large reservoir of a liquid containing the tracer. Some distance  $x$  away from this boundary the BTC is determined by a sensor. For finite times and when the outlet boundary of the porous material is sufficiently far away, we can indeed treat the system as semi-infinite, thus significantly facilitating the analytical treatment. Using the formulation in terms of a time-fractional diffusion equation and the connection between the (known) Brownian solution with its anomalous-diffusive counterpart in terms of the subordination relation, we were able to numerically analyse the concentration profile, the BTC, and the flux. For the concentration profiles and the BTC the shapes are gradually changing and thus it is difficult to extract a specific value of the anomalous diffusion exponent  $\beta$  from such data. However, we showed that the residual BTC has a power-law behaviour at sufficiently long times, allowing for a direct extraction of  $\beta$  from measurements. We also determined power-law behaviours for the tracer flux and the relative moments of the tracer mass. Both are useful when either the concentration field can be measured in single-particle tracking assays or for coloured tracers.

## Data availability statement

No new data were created or analysed in this study.

## Acknowledgments

R M acknowledges support from the German Research Foundation (DFG, Grant ME 1535/12-1). A R was partly supported by the European Union's Horizon 2020 research program under the Marie Skłodowska-Curie Grant Agreement No. 701647 and partly by the Swiss Society of Friends of the Weizmann Institute of Science. B B was supported by a research grant from the Crystal Family Foundation, the Estate of Claire Weiss, and the P. & A. Guggenheim-Ascarelli Foundation. We acknowledge the unknown Referees for their constructive comments, and for pointing out numerous additional relevant references.

## ORCID iDs

Ralf Metzler  <https://orcid.org/0000-0002-6013-7020>

Brian Berkowitz  <https://orcid.org/0000-0003-3078-1859>

## References

- [1] R Fürth (ed) 1956 *Albert Einstein: Investigations on the Theory of the Brownian Movement* (New York: Dover)
- [2] von Smoluchowski M 1906 *Ann. Phys., Lpz.* **21** 756
- [3] Nordlund I 1914 *Z. Phys. Chem.* **87** 40
- [4] Lévy P 1948 *Processus Stochastiques et Mouvement Brownien* (Paris: Gauthier-Villars)
- [5] Langevin P 1908 *C. R. Acad. Sci.* **146** 530
- [6] Lifshitz E M and Pitaevski L P 1981 *Course of Theoretical Physics 10: Physical Kinetics (Landau and Lifshitz)* (Oxford: Butterworth-Heinemann)
- [7] Brenig W 1989 *Theory of Heat: Nonequilibrium Phenomena* (Heidelberg: Springer)
- [8] Pearson K 1905 *Nature* **72** 294
- [9] Pólya G 1921 *Math. Ann.* **84** 149
- [10] Hughes B D 1995 *Random Walks and Random Environments (Random Walks vol 1)* (Oxford: Oxford University Press)
- [11] Feynman R 1964 *The Feynman Lectures of Physics vol I* (Boston, MA: Addison-Wesley)
- [12] Höfling F and Franosch T 2013 *Rep. Prog. Phys.* **76** 046602
- [13] Norregaard K, Metzler R, Ritter C, Berg-Sørensen K and Oddershede L 2017 *Chem. Rev.* **117** 4342
- [14] Scher H, Shlesinger M F and Bendler J T 1991 *Phys. Today* **44** 26
- [15] Barkai E, Garini Y and Metzler R 2012 *Phys. Today* **65** 29  
Krapf D and Metzler R 2019 *Phys. Today* **72** 48
- [16] Metzler R and Klafter J 2000 *Phys. Rep.* **339** 1–77
- [17] Sokolov I M 2012 *Soft Matter* **8** 9043
- [18] Metzler R, Jeon J-H, Cherstvy A G and Barkai E 2014 *Phys. Chem. Chem. Phys.* **16** 24128
- [19] Bouchaud J-P and Georges A 1990 *Phys. Rep.* **195** 127
- [20] Scher H and Montroll E W 1975 *Phys. Rev. B* **12** 2455
- [21] Schubert M, Preis E, Blakesley J C, Pingel P, Scherf U and Neher D 2013 *Phys. Rev. B* **87** 024203
- [22] Weigel A V, Simon B, Tamkun M M and Krapf D 2011 *Proc. Natl Acad. Sci. USA* **108** 6438
- [23] Jeon J-H, Tejedor V, Burov S, Barkai E, Selhuber-Unkel C, Berg-Sørensen K, Oddershede L and Metzler R 2011 *Phys. Rev. Lett.* **106** 048103
- [24] Chen K J, Wang B and Granick S 2015 *Nature Mater.* **14** 589
- [25] Song M S, Moon H C, Jeon J-H and Park H Y 2018 *Nat. Commun.* **9** 344
- [26] Caspi A, Granek R and Elbaum M 2000 *Phys. Rev. Lett.* **85** 5655
- [27] Gupta S, de Mel J U, Perera R M, Zolnierczuk P, Bleuel M, Faraone A and Schneider G J 2018 *J. Phys. Chem. Lett.* **9** 2956
- [28] He W, Song H, Su Y, Geng L, Ackerson B J, Peng H B and Tong P 2016 *Nat. Commun.* **7** 11701
- [29] Jeon J-H, Javanainen M, Martinez-Seara H, Metzler R and Vattulainen I 2016 *Phys. Rev. X* **6** 021006
- [30] Jeon J-H, Leijnse N, Oddershede L and Metzler R 2013 *New J. Phys.* **15** 045011
- [31] Szymanski J and Weiss M 2009 *Phys. Rev. Lett.* **103** 038102
- [32] Wu H and Schwartz D K 2020 *Acc. Chem. Res.* **53** 2130
- [33] Wu H, Wang D and Schwartz D K 2020 *J. Phys. Chem. Lett.* **11** 8825
- [34] Cherstvy A G, Thapa S, Wagner C E and Metzler R 2019 *Soft Matter* **15** 2526
- [35] Wong I Y, Gardel M L, Reichman D R, Weeks E R, Valentine M T, Bausch A R and Weitz D A 2004 *Phys. Rev. Lett.* **92** 178101
- [36] Levin M, Bel G and Roichman Y 2021 *J. Chem. Phys.* **154** 144901
- [37] Diez Fernández A, Charchar P, Cherstvy A G, Metzler R and Finnis M W 2020 *Phys. Chem. Chem. Phys.* **22** 27955
- [38] Yin C and Li X 2011 *Int. J. Pharm.* **418** 78
- [39] Freeze R A and Cherry J A 1979 *Groundwater* (Hoboken, NJ: Prentice Hall)
- [40] Domenico P A and Schwartz F W 1997 *Physical and Chemical Hydrogeology* 2nd edn (Hoboken, NJ: Wiley)
- [41] Paradisi P, Cesari R, Mainardi F and Tampieri F 2001 *Physica A* **293** 130
- [42] Compte A 1996 *Phys. Rev. E* **53** 4191
- [43] Chaves A S 1998 *Phys. Lett. A* **239** 13
- [44] Zanette D H 1998 *Physica A* **252** 159
- [45] Valdes-Parada F J, Ochoa-Tapia J A and Alvarez-Ramirez J 2007 *Physica A* **373** 339
- [46] Jiang X, Xu M and Qi H 2010 *Nonlinear Anal. Real World Appl.* **11** 262
- [47] Deng W and Barkai E 2009 *Phys. Rev. E* **79** 011112
- [48] Lutz E 2001 *Phys. Rev. E* **64** 051106
- [49] Schulz J H P, Barkai E and Metzler R 2014 *Phys. Rev. X* **4** 011028
- [50] Montroll E W 1969 *J. Math. Phys.* **10** 753
- [51] Metzler R, Barkai E and Klafter J 1999 *Phys. Rev. Lett.* **82** 3563
- [52] Metzler R, Barkai E and Klafter J 1999 *Europhys. Lett.* **46** 431
- [53] Wang W and Barkai E 2020 *Phys. Rev. Lett.* **125** 240606
- [54] Scalas E, Gorenflo R and Mainardi F 2004 *Phys. Rev. E* **69** 011107
- [55] Gorenflo R and Mainardi F 2001 *Problems in Mathematical Physics* ed J Elschner, I Gohberg and B Silbermann (Basel: Birkhäuser) p 120
- [56] Gorenflo R and Mainardi F 2003 Fractional diffusion processes: probability distributions and continuous time random walk *Processes With Long-Range Correlations (Lecture Notes in Physics vol 621)* ed G Rangarajan and M Ding (Berlin: Springer) pp 148–66
- [57] Gorenflo R, Vivoli A and Mainardi F 2004 *Nonlin. Dyn.* **38** 101
- [58] Haggerty R and Gorelick S M 1995 *Water Resour. Res.* **31** 2383
- [59] Dentz M and Berkowitz B 2003 *Water Resour. Res.* **39** 1111
- [60] Doerries T, Chechkin A V and Metzler R 2022 *J. R. Soc. Interface* **19** 20220233
- [61] Vitali S, Paradisi P and Pagnini G 2022 *J. Phys. A* **55** 224012
- [62] Maryshev B, Joelson M, Lyubimov D, Lyubimova T and Néel M-C 2009 *J. Phys. A* **42** 115001
- [63] Schumer R, Benson D A, Meerschaert M M and Baeumer B 2003 *Water Resour. Res.* **39** 1296
- [64] Doerries T J, Chechkin A V, Schumer R and Metzler R 2022 *Phys. Rev. E* **105** 014105
- [65] Wang W, Seno E, Sokolov I M, Chechkin A V and Metzler R 2020 *New J. Phys.* **22** 083041

- [66] Ślęzak J, Metzler R and Magdziarz M 2018 *New J. Phys.* **20** 023026
- [67] Vilks O et al 2022 (<https://doi.org/10.1103/PhysRevResearch.4.033055>)
- [68] Thapa S, Lomholt M A, Krog J, Cherstvy A G and Metzler R 2018 *Phys. Chem. Chem. Phys.* **20** 29018
- [69] Muñoz-Gil G, Garcia-March M A, Manzo C, Martín-Guerrero J D and Lewenstein M 2020 *New J. Phys.* **22** 013010
- [70] Muñoz-Gil G et al 2021 *Nat. Commun.* **12** 6253
- [71] Masson J-B, Casanova D, Türkcan S, Voisinne G, Popoff M R, Vergassola M and Alexandrou A 2009 *Phys. Rev. Lett.* **102** 048103
- [72] Kowalek P, Loch-Olszewska H and Szwabiński J 2019 *Phys. Rev. E* **100** 032410
- [73] Seckler H and Metzler R 2022 *Nat. Commun.* **13** 6717
- [74] Berkowitz B, Cortis A, Dentz M and Scher H 2006 *Rev. Geophys.* **44** RG2003
- [75] Berkowitz B and Scher H 2009 *Adv. Water Resour.* **32** 750
- [76] Nissan A, Dror I and Berkowitz B 2017 *Water Resour. Res.* **53** 3760
- [77] Goepfert N, Goldscheider N and Berkowitz B 2020 *Water Res.* **178** 115755
- [78] Edery Y, Guadagnini A, Scher H and Berkowitz B 2014 *Water Res. Res.* **50** 1490
- [79] Dentz M, Cortis A, Scher H and Berkowitz B 2004 *Adv. Water Resour.* **27** 155
- [80] Bijeljic B and Blunt M J 2006 *Water Resour. Res.* **42** W01202
- [81] Kirchner J W, Feng X and Neal C 2000 *Nature* **403** 524
- [82] Scher H, Margolin G, Metzler R, Klafter J and Berkowitz B 2002 *Geophys. Res. Lett.* **29** 1061
- [83] Barkai E and Cheng Y-C 2003 *J. Chem. Phys.* **118** 6167
- [84] Krüsemann H, Godec A and Metzler R 2015 *J. Phys. A* **48** 285001
- [85] Krüsemann H, Schwarzl R and Metzler R 2016 *Transp. Porous Media* **115** 327
- [86] Metzler R and Klafter J 2000 *Physica A* **278** 107
- [87] Burov S and Barkai E 2011 *Phys. Rev. Lett.* **106** 140602
- [88] Tateishi A A, Ribeiro H V, Sandev T, Petreska I and Lenzi E K 2020 *Phys. Rev. E* **101** 022135
- [89] Krom M D and Berner R A 1980 *Limnol. Oceanogr.* **25** 327–37
- [90] Bradbury M H and Green A 1985 *J. Hydrol.* **82** 39–55
- [91] Van Rees K C J, Sudicky E A, Rao P S C and Reddy K R 1991 *Environ. Sci. Technol.* **25** 1605–11
- [92] Benning J L and Barnes D L 2009 *Water Resour. Res.* **45** W09419
- [93] Podlubny I 1998 *Fractional Differential Equations* (New York: Academic)
- [94] Cairolì A, Klages R and Baule A 2018 *Proc. Natl Acad. Sci. USA* **115** 5714
- [95] Magdziarz M, Weron A and Klafter J 2008 *Phys. Rev. Lett.* **101** 210601
- [96] Feller W 1970 *An Introduction to Probability Theory and its Application* vol II (New York: Wiley)
- [97] Fogedby H C 1994 *Phys. Rev. E* **50** 1657
- [98] Klafter J and Sokolov I 2011 *First Steps in Random Walks* (Cambridge: Cambridge University Press)
- [99] Barkai E and Silbey R 2000 *J. Phys. Chem. B* **104** 3866
- [100] Dentz M, Cortis A, Scher H and Berkowitz B 2004 *Adv. Wat. Res.* **27** 155
- [101] Klemm A, Metzler R and Kimmich R 2002 *Phys. Rev. E* **65** 021112
- [102] Skaug M J, Wang L, Ding Y and Schwartz D K 2015 *ACS Nano* **2** 2148
- [103] Mathematica version 13.0.1 (Champaign, IL: Wolfram Research)